Energy Engineering

Tech Science Press

DOI: 10.32604/ee.2023.028898

ARTICLE

Effects of I-EGR and Pre-Injection on Performance of Gasoline Compression Ignition (GCI) at Low-Load Condition

Binbin Yang[1,*], Leilei Liu[1], Yan Zhang[1], Jingyu Gong[1], Fan Zhang[2] and Tiezhu Zhang[1]

[1]School of Transportation and Vehicle Engineering, Shandong University of Technology, Zibo, 255000, China

[2]State Key Laboratory of Engines, Tianjin University, Tianjin, 300072, China

[*]Corresponding Author: Binbin Yang. Email: yangbinbin@sdut.edu.cn

Received: 14 January 2023 Accepted: 15 May 2023 Published: 28 September 2023

ABSTRACT

Gasoline compression ignition (GCI) has been considered as a promising combustion concept to yield ultra-low NO_X and soot emissions while maintaining high thermal efficiency. However, how to improve the low-load performance becomes an urgent issue to be solved. In this paper, a GCI engine model was built to investigate the effects of internal EGR (i-EGR) and pre-injection on in-cylinder temperature, spatial concentration of mixture and OH radical, combustion and emission characteristics, and the control strategy for improving the combustion performance was further explored. The results showed an obvious expansion of the zone with an equivalence ratio between 0.8∼1.2 is realized by higher pre-injection ratios, and the s decreases with the increase of pre-injection ratio, but increases with the increase of i-EGR ratio. The high overlap among the equivalent mixture zone, the high-temperature zone, and the OH radical-rich zone can be achieved by higher i-EGR ratio coupled with higher pre-injection ratio. By increasing the pre-injection ratio, the combustion efficiency increases first and then decreases, also achieves the peak value with a pre-injection ratio of 60% and is unaffected by i-EGR. The emissions of CO, HC, NO_X, and soot can also be reduced to low levels by the combination of higher i-EGR ratios and a pre-injection ratio of 60%.

KEYWORDS

Gasoline compression ignition; low-load condition; internal EGR; pre-injection; combustion characteristics; emissions

Nomenclature

AMR	Adaptive mesh refinement
ATDC	After top dead center
CA10	The crank angle degree at which 10% of total heat release has taken place
CFD	Computational fluid dynamics
CI	Compression ignition
CO	Carbon monoxide
CO_2	Carbon dioxide
EGR	Exhaust gas recirculation
EVC	Exhaust valve closing
EVO	Exhaust valve opening
GCI	Gasoline compression ignition

H_2	Hydrogen
HC	Hydrocarbon
ICE	Internal combustion engine
IC_8H_{18}	Iso-octane
i-EGR	Internal exhaust gas recirculation
IVC	Intake valve closing
IVO	Intake valve opening
LHV	Lower heating value
NC_7H_{16}	N-heptane
NO_X	Nitrogen oxide
NTC	No. time counter
OH	Hydroxyl
PRF	Primary reference fuel
RNG	Renormalized group
rpm	Revolutions per minute
SI	Spark ignition
TDC	Top dead center

1 Introduction

Currently, faced with the increasingly severe energy and environmental issues, both developed and developing countries have accelerated their efforts to better the industry and energy structures, so as to reduce carbon dioxide (CO_2) emissions significantly. The Chinese government has already committed to peak CO_2 emission before 2030 and achieve carbon neutrality before 2060. Thus, the carbon reduction in the transportation sector, which is responsible for 20% of the total carbon emission, is essential to the success of carbon peaking and carbon neutrality goals. Researchers have attempted to develop vehicles with alternative powertrains, for example, hybrid electric vehicles (HEVs) [1,2], battery electric vehicles (BEVs) [3–5], and fuel cell vehicles (FCVs) [6,7], in order to alleviate the dependence on fossil fuels. But as the major power plant of transportation, internal combustion engines (ICEs) are expected to deliver approximately 90% of the total energy even by 2040 [8], and have a widespread application in the fields of micro power conversion, as well as high power output such as the heavy-duty engines in power station [9].

Compression ignition (CI) engine has superior efficiency characteristics as compared to spark ignition (SI) engine, in spite of this, the massive emissions of NO_X and soot produced in diesel combustion become a subject of social and academic concern [10]. In recent years, several researchers focus on solving the issues from the perspectives of advanced combustion concept and biofuel [11–14]. In an attempt to diminish engine-out pollution, Kalghatgi et al. [15,16] have proposed injecting gasoline fuel directly into the cylinder by a common-rail system to achieve partially premixed combustion, also referred to as gasoline compression ignition (GCI). GCI combustion allows the sufficient premixing of gasoline and fresh air intake [17], coupled with the proper combustion phasing and heat release rate via, for instance, multiple injections and moderate exhaust gas recirculation (EGR), resulting in ultra-low NO_X and soot emissions along with the comparable thermal efficiency to traditional CI engines [15–23]. However, due to the high octane number, namely the low reactivity of gasoline, the GCI operation under low loads is prone to experience problems in the ignition, combustion stability, and incomplete combustion products, even misfire in some cases [18,19]. To address these issues, several existing technologies have been applied, mainly including intake preheating, intake boosting, multi-injection, and internal EGR (i-EGR).

The increasing of intake temperature and pressure is considered to be the most direct technical mean for improving the initial thermodynamics state of the in-cylinder charge and can accelerate the flame propagation rate after ignition. In the last two decades, a series of experimental and modeling studies have been performed to assess the auto-ignition characteristics of GCI combustion. According to the experimental studies by Weall et al. [24] and Xiao et al. [25], once the intake temperature exceeds a certain value, the low-load limits of stable combustion can be extended to 0.1 MPa BMEP and 0.1 MPa IMEP, respectively, and the more complete combustion and the higher thermal efficiency can be obtained as well. Solaka et al. [26] demonstrated that, through increasing λ by means of extended boosting with an EGR ratio fixed, the fuels with various octane values could be operated down to 0.2 MPa IMEP. The effects of intake preheating and boosting have been investigated by Jiang et al. [27] on a modified single-cylinder engine. Except for the positive impact of the favorable intake conditions on thermal efficiency and combustion stability, the increased intake temperature helps to reduce the total particle number slightly. Nonetheless, the thermal lag and extra energy consumption greatly limit the practical application of these two techniques.

Employing multiple injections usually improves the fuel-air mixing, and contributes to lower the cyclic variations of GCI combustion within the controlled range. The sensitivity of combustion stability has been studied by An et al. [28] on a fully transparent optical engine. The results showed multi-injection strategy can be employed to reduce the minimum intake air temperature for stable GCI operation from 70°C (single injection) to 50°C, and the more stable combustion is obtained as the injection pressure is increased to 80 MPa. By means of electronically excited hydroxyl (OH) imaging, Goyal et al. [29] demonstrated that, as compared to single injection, the process of flame merging of double-injection based GCI combustion is more advanced, and the flame propagation rate is also accelerated, both of which exhibit significant contribution to ignition kernel development. Liu et al. [30] found in the experimental study that, the pilot gasoline fuel with low injection pressure is more ignitable than that with high injection pressures. In a recent study by Wang et al. [31], the pre-injection can effectively decrease the mixture inhomogeneity and increase the OH radical concentration during the main combustion, which can promote the combustion reaction, thereby reducing the possibility of combustion instability. In addition, the combustion temperature can be increased to promote the oxidation of CO and HC.

I-EGR appears to be a promising approach easy to be realized for improving the ignition property because the initial thermodynamic state of the in-cylinder mixture can be effectively controlled by residual gas. Moreover, the oxidation reaction (without ignition) of gasoline with the increased temperature produces highly reactive molecules, such as O, H, and OH, which act as catalysts for spontaneous ignition. However, the excessive i-EGR cannot be allowed owing to its negative impact on oxygen concentration. Zhang et al. [32] realized the exhaust valve reopening (2-EVO) by electro-hydraulic variable valve system and came to a conclusion that the stable GCI combustion can be carried out with 0.15 MPa IMEP, while a maximum indicated thermal efficiency over 40% has been achieved using both intake boosting and flexible fuel injection strategy. Zhou et al. [33,34] demonstrated the combination of i-EGR, fuel reforming, and intake preheating is an effective approach to improve combustion stability and cold-start performance of GCI engines, while the heating effect of i-EGR plays the dominant role during idling condition.

In summary, the conditions favorable for ignition, such as the mixture stratification and the OH radical by multiple injections, as well as the better initial thermodynamic state and the fuel reforming by i-EGR have been intensely researched. However, these factors are usually considered separately, and much is still unknown about the detailed combustion behavior by the cooperative control of pre-injection and i-EGR. In the CFD simulation has been conducted by Zhu et al. [35],

the preferable combination of equivalent mixture and high temperature essentially plays a role in improving combustion efficiency and thermal efficiency. Thus, it can be inferred the high contact among the equivalent mixture zone, the high-temperature zone, and the OH radical-rich zone is likely to be the subject of a more promising solution for stable combustion. Therefore, the objective of the current investigation is first to define the mixture stratification quantitatively and clarify the coupling influence of i-EGR and pre-injection on in-cylinder temperature, mixture, and OH radical concentration spatially, as well as combustion and emission characteristics, further exploring the control strategy for improving the performance of GCI combustion at low loads.

2 Numerical Approaches

2.1 Computational Grid and Models

Multidimensional CFD simulation was performed using CONVERGE 2.3 software to simulate the low-load operation of GCI combustion, and the computational grid with intake and exhaust ports at TDC is shown in Fig. 1. The basic mesh of the grid was 4.0 mm, and the region of the combustion chamber was locally encrypted to 1.0 mm for detailed calculation by adaptive mesh refinement (AMR), thus the grid number reached around 95000. Simulations with other grid resolutions have been conducted to confirm that the results were adequately grid-independent [35]. The sub-models used in the simulation are shown in Table 1.

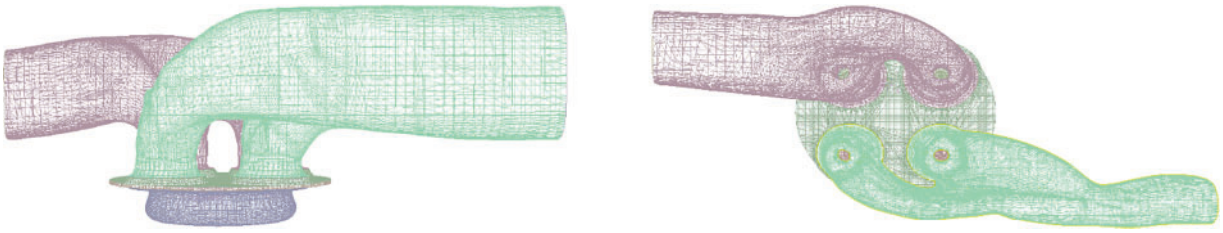

Figure 1: Computational grid with intake and exhaust ports at TDC

Table 1: Computational model and mechanism

Turbulence model	Renormalized group (RNG) k-ε model [36]
Turbulent diffusion model	O'Rourke model [37]
Spray evaporation model	Frossling model [38]
Droplet breakup model	KH-RT model [39]
Droplet collision and coalescence model	No. time counter (NTC) model [40]
Droplet drop/wall interaction model	Rebound/slide model [41]
Combustion model	SAGE detailed chemical kinetic model [42]
Chemical reaction mechanism	PRF mechanism [43]
NO_X mechanism	Zeldovich NO_X mechanism [44]
Soot mechanism	Hiroyasu NSC soot generation and oxidation mechanism [45]

The engine and injector specifications are shown in Table 2, and the operation conditions are shown in Table 3. The experimental data of in-cylinder pressure and heat release rate came from the single-injection experiment (1500 rpm @ 0.5 MPa IMEP) on the modified single-cylinder CI engine. The comparison of in-cylinder pressure and heat release rate profiles between experimental and simulation results is shown in Fig. 2, which indicates the prediction of the simulation is within acceptable limits.

Table 2: Engine and injector specifications

Parameter	Value
Displacement [L]	1.08
Compression ratio	16:1
Bore [mm]	105
Stroke [mm]	125
Connecting rod length [mm]	210
IVO [°CA ATDC]	−377
IVC [°CA ATDC]	−133
EVO [°CA ATDC]	125
EVC [°CA ATDC]	197
Number of holes	8
Hole diameter [mm]	0.15
Cone angle [°]	150

Table 3: Engine operation conditions

Parameter	Value
Speed [rpm]	1500
Intake pressure [MPa]	0.104
Intake temperature [K]	303
Fuel injection quantity [mg/cycle]	20
Injection pressure [MPa]	50
Pre-injection timing [°CA ATDC]	−60
Main-injection timing [°CA ATDC]	−15

2.2 Parameter Declaration

In this study, i-EGR was realized by the 2-EVO strategy while the intake valve timing was fixed during the operation, as the lift curves of the intake and exhaust valves shown in Fig. 3. The definition of i-EGR ratio is shown in Eq. (1).

$$R_{EGR} = \frac{m_{tot} - m_{air}}{m_{tot}} \tag{1}$$

where, m_{tot} is the total mass of in-cylinder charge at the end of the intake stroke, m_{air} is the mass of fresh air intake. Under the 2-EVO strategy, as the opening degree of the back pressure valve is decreased, more residual gas will be trapped in the cylinder, which results in the increase of the i-EGR ratio.

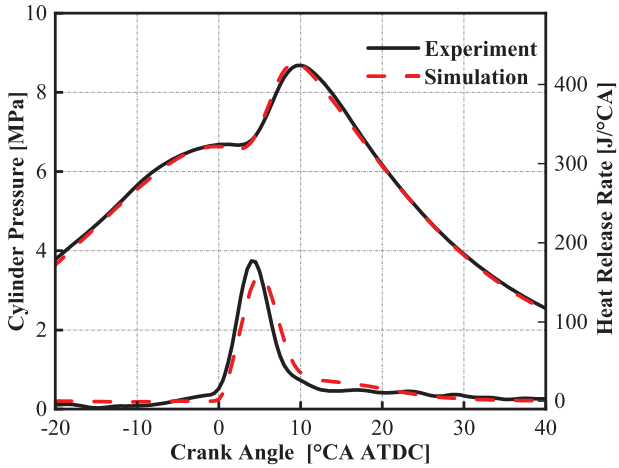

Figure 2: Model verification

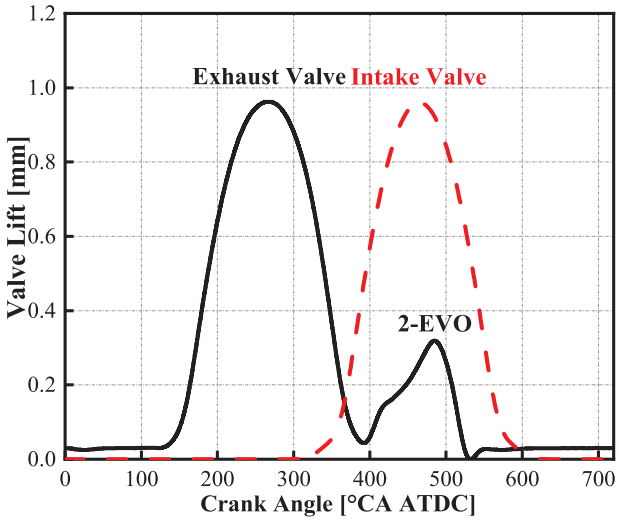

Figure 3: Valve lift profiles

In order to analyze the mixture concentration distribution quantitatively, a weighted average of the equivalence ratio of each mesh was carried out, and the average equivalence ratio ϕ was obtained by Eq. (2).

$$\phi = \frac{\sum_{i=1}^{n} \phi_i V_i}{\sum_{i=1}^{n} V_i} \tag{2}$$

where, ϕ_i and V_i are the equivalence ratio and the volume of each mesh, respectively. The standard deviation of equivalence ratio distribution was defined in Eq. (3). As the mixture concentration distribution in the cylinder is more uniform, the local equivalence ratio is closer to the mean value, namely, the dispersion s is smaller.

$$s = \sqrt{\frac{1}{V_{tot}} \sum_{i=1}^{n} (\phi_i - \phi)^2 V_i} \tag{3}$$

where, V_{tot} is the volume of the cylinder (m^3).

Combustion efficiency was defined as the ratio of the actual heat released to the one by complete combustion, as shown in Eq. (4).

$$\eta_{comb} = \left(1 - \frac{\sum_{i=1}^{n} x_i Q_{LHV_i}}{Q_{LHV_{fuel}}}\right) \times 100\% \tag{4}$$

where, x_i and Q_{LHV_i} are the mass fractions and lower heating value of incomplete combustion products, including CO, HC, and hydrogen (H_2), $Q_{LHV_{fuel}}$ is the lower heating value of the fuel. For this study, Q_{LHVHC} has been treated equally to $Q_{LHV_{fuel}}$.

3 Results and Discussion

3.1 Mixing and Combustion Characteristics

The in-cylinder pressure and heat release rate profiles under various i-EGR ratios (20%, 30%, 40%, 50%, and 60%) and pre-injection ratios (0%, 20%, 40%, 60%, 80%, and 100%) are shown in Fig. 4. It is clear that, as an i-EGR ratio of 20% is used, the heat release is relatively retarded while the combustion process deteriorates with the increase of pre-injection ratio gradually, resulting in misfire at last. This is because the thermodynamic state improvement of the in-cylinder charge caused by the lower i-EGR ratio is insufficient for stable GCI combustion under the current condition, especially for the globally over-uniform mixture by a higher pre-injection ratio. Thus the case with an i-EGR ratio of 20% will not be discussed in the following sections. As the i-EGR ratio is raised to 30%, the combustion process is slightly improved due to the better thermal atmosphere by more trapped hot residual gas, but the overall trend with increasing pre-injection ratio is largely unchanged. As far as the i-EGR ratio reaches 40%, the peak values of both in-cylinder pressure and heat release rate display a definite trend of increasing first and then decreasing with the increase of the pre-injection ratio. When the pre-injection ratio is 50%, the peak in-cylinder pressure arrives at the maximum value, while the heat release process shows a similar trend with the last case, and the combustion duration is shortened first and then increased. This phenomenon can be explained by the fact that, with the increase of pre-injection ratio, the in-cylinder charge is more uniform that the flame development in the typical multi-point ignition of GCI combustion [46] is significantly improved, thus the heat release process tends to be more concentrated. However, the local mixture in the cylinder is too lean to maintain stable flame propagation, resulting in incomplete combustion. Meanwhile, as the i-EGR ratio exceeds 50%, the in-cylinder temperature is increased evidently due to the sufficient hot residual gas by i-EGR, which promotes the ignition and flame propagation in the lean mixture regions, thus the combustion process is no longer deteriorated by high pre-injection ratios.

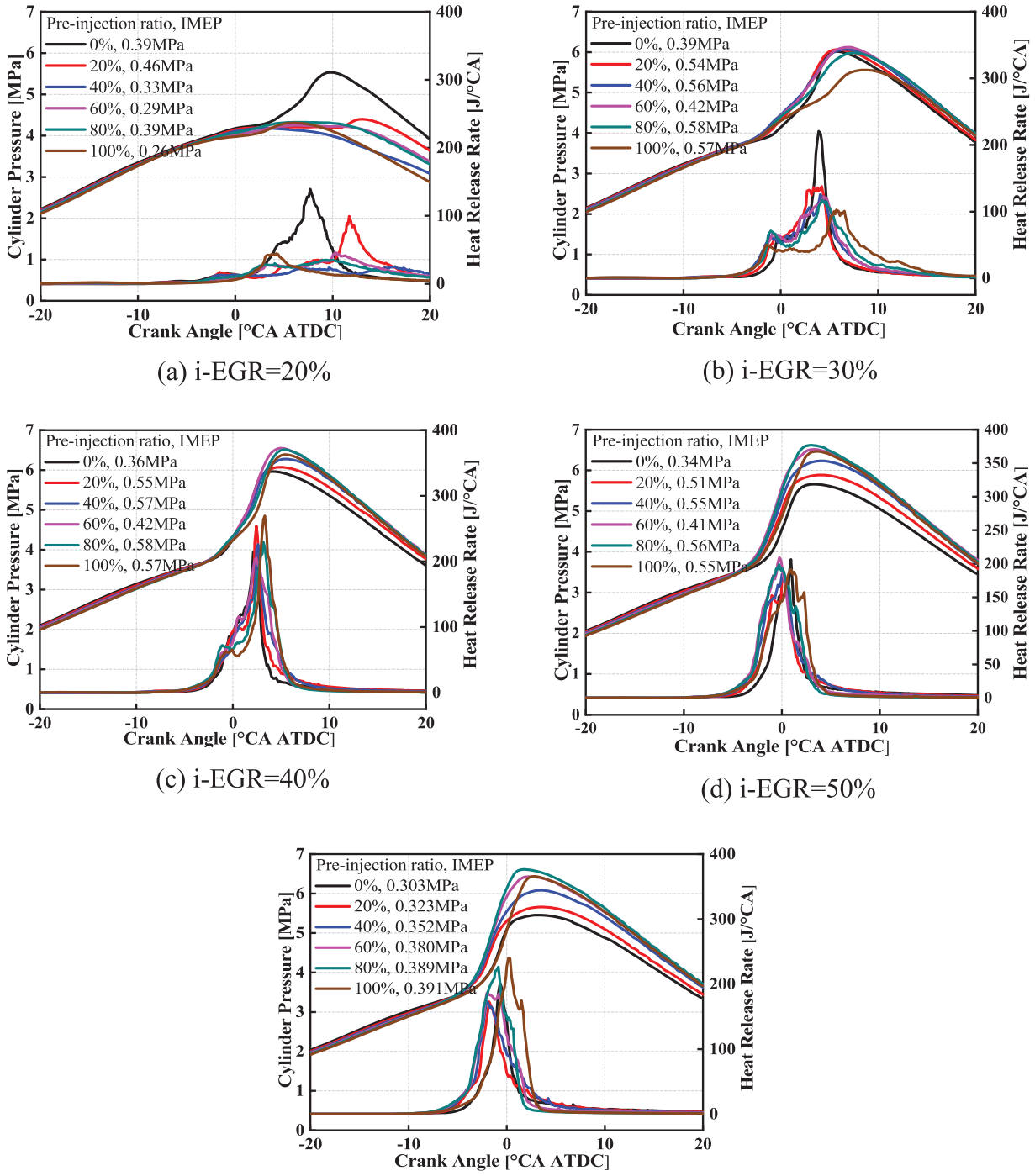

Figure 4: In-cylinder pressure and heat release rate profiles with various i-EGR and pre-injection ratios

Fig. 5 shows the effects of i-EGR and pre-injection on the distribution and the *s* of equivalence ratio at CA10 (the crank angle degree at which 10% of total heat release has taken place). As illustrated

in the histogram, the volume ratios of mixture with equivalence ratio between 0.8 and 1.2 expand obviously, and the *s* of equivalence ratio tends to decrease because of the more homogeneous charge by injecting more fuel in the early stage of the compression stroke. With the increasing i-EGR ratio, the regions of the extremely lean mixture ($\Phi = 0 \sim 0.4$) decrease gradually. This is mainly because the oxygen concentration is reduced due to the dilution effect of i-EGR with the fuel injection quantity fixed, also resulting in an overall increase of equivalence ratio in the cylinder. Moreover, the start of combustion is advanced owing to the addition of i-EGR, and the ignition delay is reduced accordingly, which leads to the enhanced degree of mixture stratification, represented as the *s* of equivalence ratio under various i-EGR ratios.

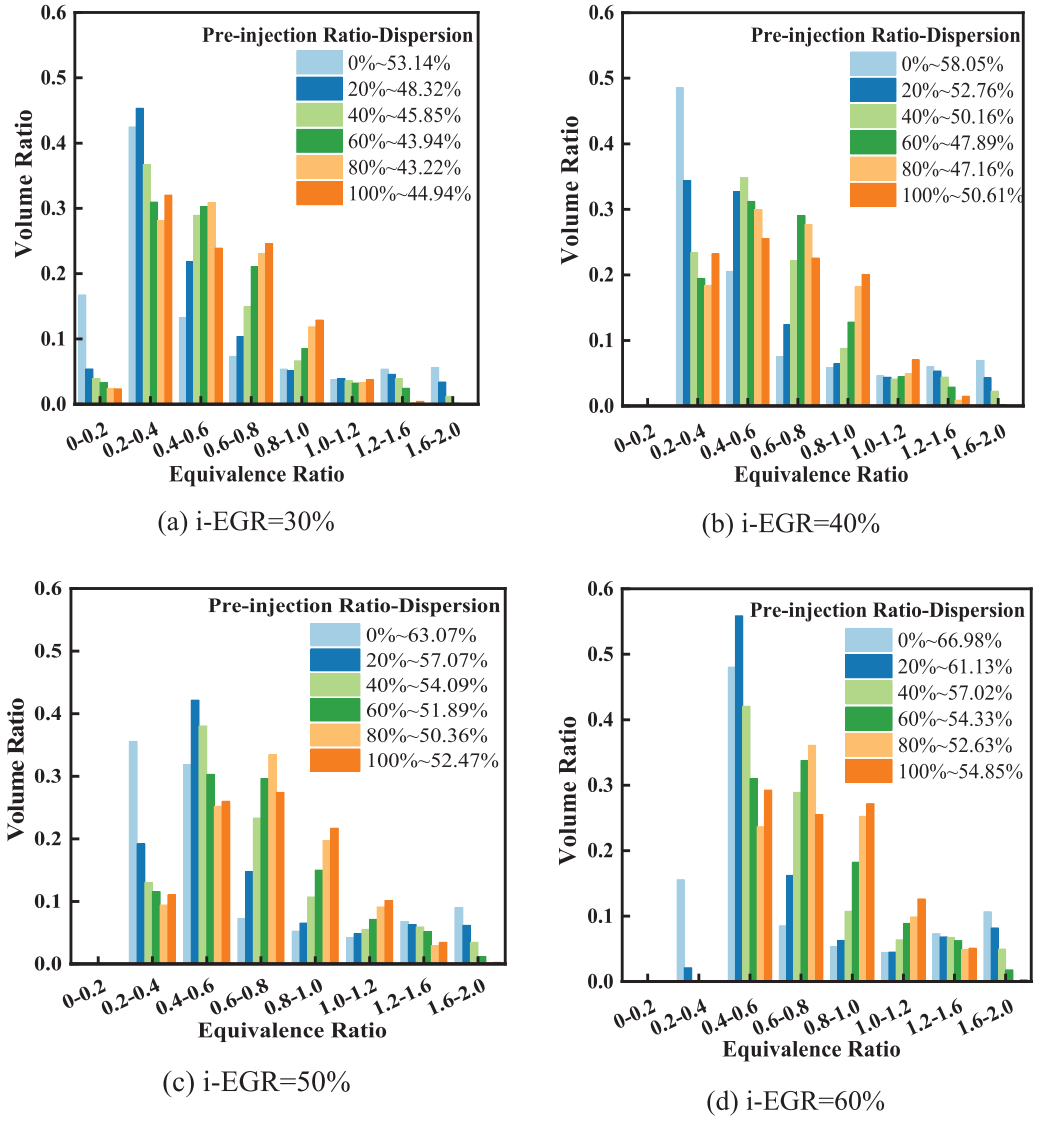

Figure 5: Effects of i-EGR and pre-injection on distribution and *s* of equivalence ratio at CA10

Fig. 6 shows the plan view of the flow field in the cylinder under various i-EGR ratios without pre-injection. As the increase of i-EGR by higher back pressure, the in-cylinder flow is greatly affected

by exhaust valve rebreathing. Under the condition with an i-EGR ratio of 30%, the flow velocity in the center of combustion is higher than that of other areas. It is worth noting that, an obvious flow from the regions near intake valves to the areas close to exhaust valves begins to appear as i-EGR ratio higher than 40%. Meanwhile, the flow velocity in surrounding areas is enhanced, but that in the center of the combustion chamber is reduced obviously.

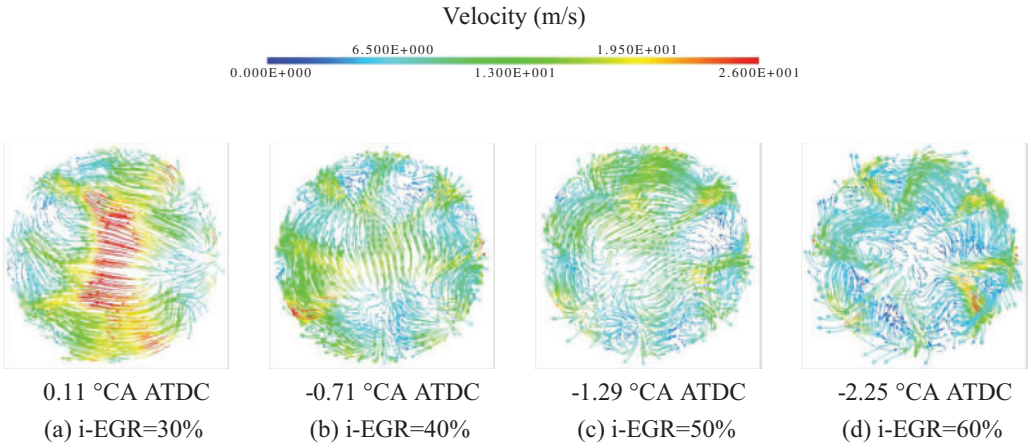

Figure 6: In-cylinder flow fields under various i-EGR ratios without pre-injection (bottom: intake valves, top: exhaust valves)

Fig. 7 shows the distribution of mixture concentration represented by the equivalence ratio at CA10 under various i-EGR ratios and pre-injection ratios. As a result of the in-cylinder flow from the regions near intake valves to the areas close to exhaust valves as shown in Fig. 6, as well as the more residual gas trapped by i-EGR, the mixture concentration in the region near exhaust valves increases significantly. Under the circumstances without pre-injection, the fuel spray with long penetration is directly injected into the wall of the combustion chamber and deposited at the bottom, where the mixture concentration is extremely high. Similar to the results shown in Fig. 5, the increasing pre-injection ratio yields greater uniformity of the in-cylinder mixture, thus the locally over-rich regions near the wall disappear gradually and the equivalent mixture zone expands evidently. Under such condition, the mixture is mainly concentrated in the center of the combustion chamber, but more and more fuel enters into the squish area, which is likely to result in higher incomplete combustion products.

Fig. 8 shows the distribution of in-cylinder temperature at CA10 under various i-EGR ratios and pre-injection ratios. It is evident that, owing to the more uniform mixture by higher pre-injection ratio, the distribution of in-cylinder temperature also becomes more homogeneous, and the locally high-temperature regions decrease as well. However, as a result of the heating effect by residual gas, the high-temperature zone near exhaust valves becomes larger by higher i-EGR ratios. Thus, through higher i-EGR ratios coupled with higher pre-injection ratios, the high-temperature zone is highly overlapped with the equivalent mixture zone.

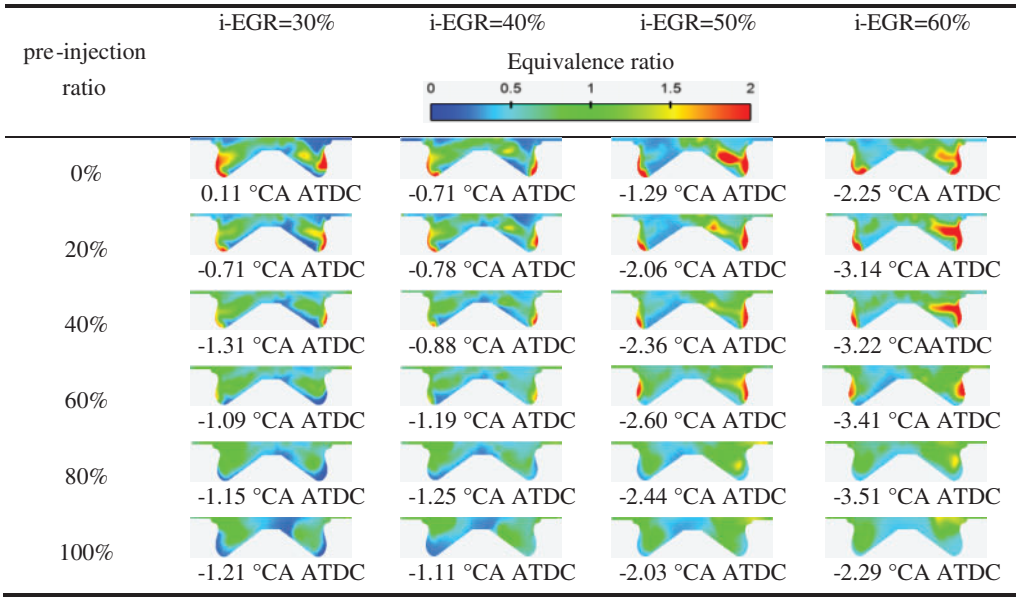

Figure 7: Mixture concentration distribution at CA10 with various i-EGR and pre-injection ratios (left: intake valves, right: exhaust valves)

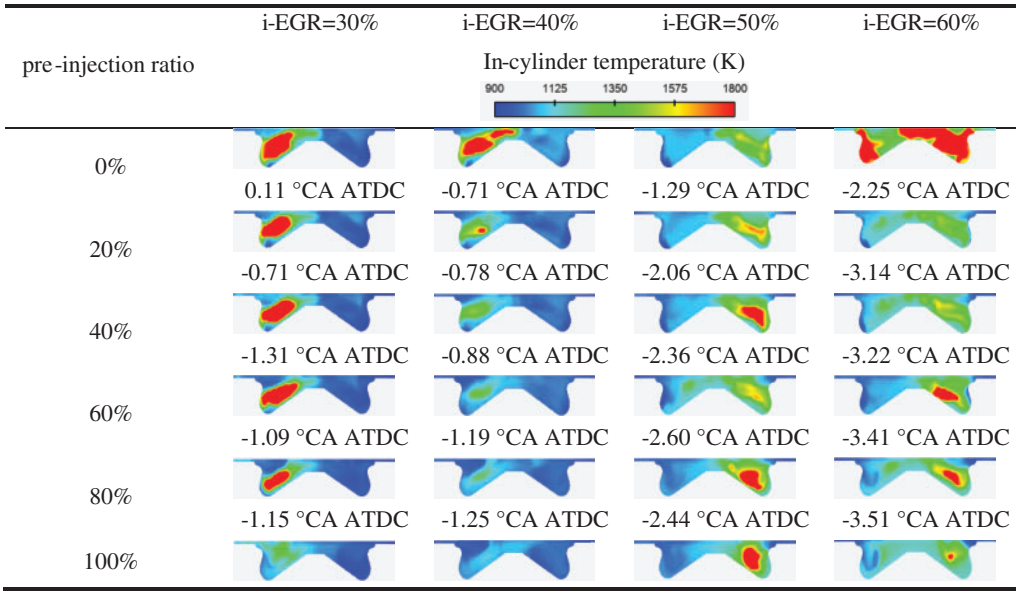

Figure 8: In-cylinder temperature distribution at CA10 with various i-EGR and pre-injection ratios (left: intake valves, right: exhaust valves)

Fig. 9 shows the distribution of OH radicals at CA10 under various i-EGR ratios and pre-injection ratios. As the main product of low-temperature reaction, the distribution of OH radicals has a certain correlation with the mixture concentration, that is, the concentration of OH radicals in the regions near exhaust valves is gradually increased with higher i-EGR ratio. Besides, the rapid consumption of OH radicals has a significant impact on flame propagation. Thus, the variation of the OH radical

distribution can also explain why the in-cylinder temperature is reduced as the i-EGR ratio raised from 30% to 40% shown in Fig. 8. However, once the i-EGR ratio reaches 60%, the OH radical concentration is much lowered, since the dilution effect by residual gas on oxygen concentration plays a major role, which inhabits the low-temperature reaction of fuel from producing OH radical. Therefore, based on the results shown in Figs. 7–9, as the combination of higher i-EGR ratio and higher pre-injection ratio is used, there is a high contact among the equivalent mixture zone, the high-temperature zone, and the OH radical-rich zone in the center of the combustion chamber near exhaust valves, which will be beneficial for the subsequent combustion process.

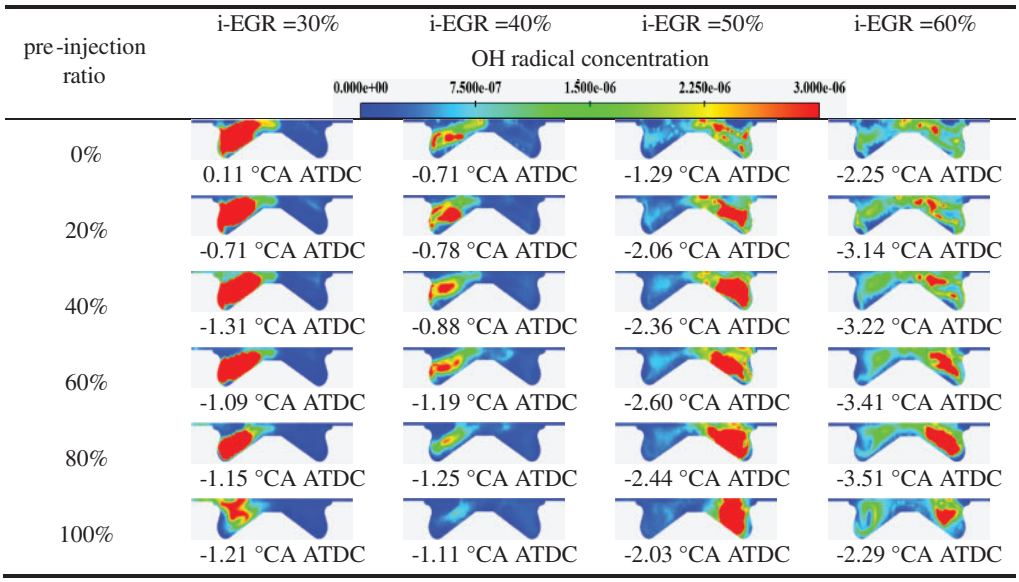

Figure 9: OH radical concentration distribution at CA10 with various i-EGR and pre-injection ratios (left: intake valves, right: exhaust valves)

Fig. 10 shows the effects of i-EGR and pre-injection on combustion efficiency. With the i-EGR ratios of 30%, 40%, 50%, and 60%, the combustion efficiency increases first and then decreases by increasing the pre-injection ratio, and the peak combustion efficiency of more than 97% can be obtained with the pre-injection ratio of 60%. When the i-EGR ratio is 30%, the improvement of combustion efficiency by a higher pre-injection ratio is less obvious. As the i-EGR ratio is raised from 40% to 60%, a downward trend in combustion efficiency is observed. As shown in Fig. 7, the higher pre-injection ratio makes more fuel enter the squish area of the combustion chamber when the lower i-EGR ratios are used, leading to more incomplete combustion. However, due to the better thermal atmosphere in the cylinder resulting from a higher i-EGR ratio, the effect of fuel trapped in the squish area on the combustion process becomes less significant.

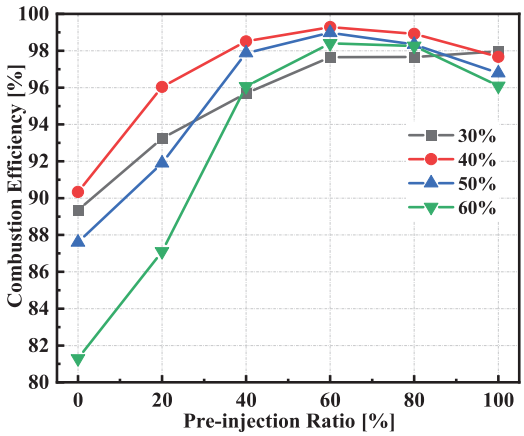

Figure 10: Effects of i-EGR and pre-injection on combustion efficiency

3.2 Emission Characteristics

Figs. 11 and 12 show the effects of i-EGR and pre-injection on CO and HC emissions, respectively. Within the i-EGR ratio range between 40% and 60%, the emissions of CO and HC show an overall decline trend by increasing the pre-injection ratio but slightly increase with the pre-injection ratio of 100%. Moreover, they are almost lower than 10 and 0.2 g/kWh respectively when the pre-injection ratio is between 40% and 80%. The observed reduction of CO and HC emissions is due to the fact that, by injecting more fuel in the early stage, though more fuel enters into the squish area, the fuel near the wall of the combustion chamber is reduced obviously, and the *s* of the in-cylinder charge decreases. Moreover, the higher degree of overlap among the equivalent mixture zone, the high-temperature zone, and the OH radical-rich zone is obtained by the increased pre-injection ratio, as shown in Figs. 7–9, which improves the combustion performance. Once the pre-injection ratio reaches 40%, CO and HC emissions remain essentially unchanged with various i-EGR ratios. However, as the i-EGR ratio of 30% is used, both the oxygen concentration and the wall temperature are lower, producing more CO and unburned HC.

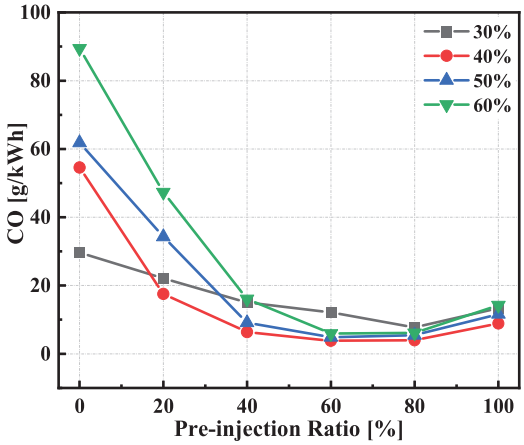

Figure 11: Effects of i-EGR and pre-injection on CO emission

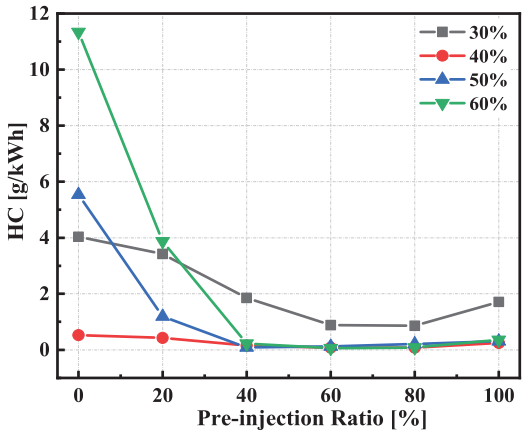

Figure 12: Effects of i-EGR and pre-injection on HC emission

Fig. 13 shows the effects of i-EGR and pre-injection on NO_X emission. Under low load conditions, the overall low NO_X emission (below 1 g/kWh) can be achieved owing to the low combustion temperature, and the influence of pre-injection ratio on NO_X emission is not evident. Also, it is worth noting that there is a wave crest for each i-EGR ratio when the pre-injection ratio is around 60%. This is mainly because, the area of the high-temperature zone with the pre-injection ratio of 60% is obviously larger than that in the other cases as shown in Fig. 8, which helps to generate more NO_X. As the i-EGR ratio is increased, the combination of dilution and specific heat effects of residual gas leads to an obvious reduction of oxygen concentration and peak combustion temperature, which has a higher impact on NO_X generation than the heating effect of i-EGR, thus the NO_X emission with lower pre-injection ratios is reduced.

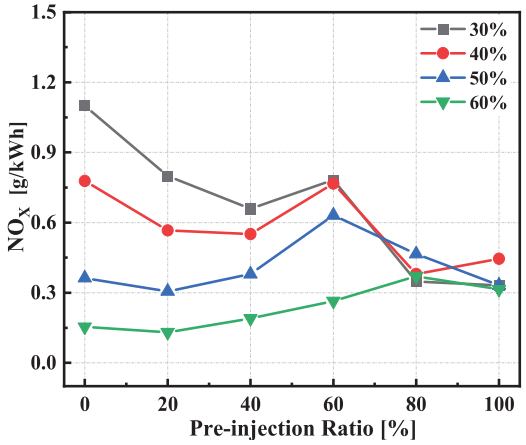

Figure 13: Effects of i-EGR and pre-injection on NO_X emission

Fig. 14 shows the effects of i-EGR and pre-injection on soot emission. It is found that within the i-EGR ratio range between 30% and 60%, soot emission shows a decreasing trend with a higher pre-injection ratio, and can be reduced to below 0.1 g/kWh. This is mainly because soot is usually generated in the locally rich region, such as the flame center, as well as the low-temperature regions near the wall, while a large proportion of fuel is injected early into the cylinder, the sufficient premixing allows the

mixture to be more homogenous and the locally fuel-rich regions are greatly reduced. However, due to the higher oxygen concentration with the i-EGR ratio of 30%, it is likely to generate less soot emission despite the lower combustion temperature because of the weakened condensation and polymerization process of soot precursors. As the i-EGR ratio increases, the phenomenon disappears gradually due to the weakened mixture stratification by a higher pre-injection ratio, and the equivalent mixture zone is more overlapped with the high-temperature zone, as shown in Figs. 7 and 8, promoting the late oxidation process of soot effectively.

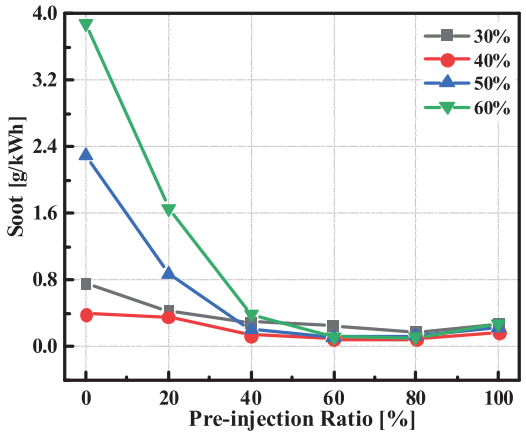

Figure 14: Effects of i-EGR and pre-injection on soot emission

Based on the above analysis, as compared with the single-injection case (pre-injection ratio = 0%), the double-injection is well situated to lower the emissions. Besides, quasi-HCCI combustion (pre-injection ratio = 100%) generates a little higher CO, HC, and soot emissions owing to the more uniform charge, while the NO_X emission is comparable to other conditions. Thus, it can be said that the optimized emissions of main pollution can be achieved by higher i-EGR ratios coupled with the pre-injection ratio of 60% under low-load conditions.

4 Conclusions

In the current research, numerical simulation has been conducted to investigate the effects of i-EGR and pre-injection on the low-load operation of GCI combustion, and the dispersion of the equivalent ratio has also been defined. The detailed conclusions are summarized as follows:

1. The combination of higher i-EGR ratio and higher pre-injection ratio is helpful for achieving the high contact among the equivalent mixture zone, the high-temperature zone, and the OH radical-rich zone in the cylinder. This allows for optimized combustion and emission performance, which may be a key issue in improving the combustion stability of GCI combustion under low loads.

2. With the increase of pre-injection ratio, the area of equivalence ratio between 0.8∼1.2 expands obviously, and the s of the in-cylinder charge tends to decrease. With the increase of i-EGR ratio, the proportion of lean mixture decreases, and the mixture stratification is enhanced.

3. By increasing the pre-injection ratio, the combustion efficiency shows an overall trend of increasing first and then decreasing, and a peak value higher than 97% is obtained with the pre-injection ratio of 60% regardless of the i-EGR ratio.

4. CO, HC, and soot emissions are reduced by higher pre-injection ratios but show a slight rise with the pre-injection ratio of 100%, while i-EGR has little impact on them under the cases with the pre-injection ratio higher than 40%. With the lower pre-injection ratios, NO_X emission can be decreased by higher i-EGR ratios, as well as is basically unaffected by i-EGR with the pre-injection ratio higher than 80% and remains at low levels.

Acknowledgement: The authors acknowledge the reviewers for providing valuable comments and helpful suggestions to improve the manuscript.

Funding Statement: This study is sponsored by the projects of National Natural Science Foundation of China (Grant Nos. 51806127 and 52075307) and Key Research and Development Program of Shandong Province (Grant No. 2019GHZ016).

Author Contributions: Study conception and design: Binbin Yang; data collection: Jingyu Gong, Fan Zhang; analysis and interpretation of results: Leilei Liu, Yan Zhang; draft manuscript preparation: Leilei Liu, Jingyu Gong; validation, writing-review and editing: Binbin Yang; supervision: Tiezhu Zhang. All authors reviewed the results and approved the final version of the manuscript.

Availability of Data and Materials: Data will be made available on request.

Conflicts of Interest: The authors declare that they have no conflicts of interest to report regarding the present study.

References

1. Saiteja, P., Ashok, B. (2022). Critical review on structural architecture, energy control strategies and development process towards optimal energy management in hybrid vehicles. *Renewable and Sustainable Energy Reviews, 157(1),* 112038.
2. Bai, S., Liu, C. (2021). Overview of energy harvesting and emission reduction technologies in hybrid electric vehicles. *Renewable and Sustainable Energy Reviews, 147(1),* 111188.
3. Li, Z., Khajepour, A., Song, J. (2019). A comprehensive review of the key technologies for pure electric vehicles. *Energy, 182(4),* 824–839.
4. Ibrahim, A., Jiang, F. (2021). The electric vehicle energy management: An overview of the energy system and related modeling and simulation. *Renewable and Sustainable Energy Reviews, 144(268),* 111049.
5. Tete, P. R., Gupta, M. M., Joshi, S. S. (2021). Developments in battery thermal management systems for electric vehicles: A technical review. *Journal of Energy Storage, 35,* 102255.
6. İnci, M., Büyük, M., Demir, M. H., İlbey, G. (2021). A review and research on fuel cell electric vehicles: Topologies, power electronic converters, energy management methods, technical challenges, marketing and future aspects. *Renewable and Sustainable Energy Reviews, 137(12),* 110648.
7. Lü, X., Wu, Y., Lian, J., Zhang, Y., Chen, C. et al. (2020). Energy management of hybrid electric vehicles: A review of energy optimization of fuel cell hybrid power system based on genetic algorithm. *Energy Conversion and Management, 205(22),* 112474.
8. Kalghatgi, G., Levinsky, H., Colket, M. (2018). Future transportation fuels. *Progress in Energy and Combustion Science, 69,* 103–105.
9. Araghi, Y., Kroesen, M., Wee, B. (2017). Identifying reasons for historic car ownership and use and policy implications: An explorative latent class analysis. *Transport Policy, 56(2),* 12–18.
10. Dec, J. E. (2009). Advanced compression-ignition engines-understanding the in-cylinder processes. *Proceedings of the Combustion Institute, 32(2),* 2727–2742.

11. Ganesan, N., Le, T. H., Ekambaram, P., Balasubramanian, D., Le, V. V. et al. (2022). Experimental assessment on performance and combustion behaviors of reactivity-controlled compression ignition engine operated by n-pentanol and cottonseed biodiesel. *Journal of Cleaner Production, 330,* 129781.
12. Cao, D. N., Hoang, A. T., Luu, H. Q., Bui, V. G., Tran, T. T. H. (2020). Effects of injection pressure on the NOx and PM emission control of diesel engine: A review under the aspect of PCCI combustion condition. *Energy Sources, Part A: Recovery, Utilization, and Environmental Effects, 15,* 1–18.
13. Hoang, A. T., Tran, Q. V., Al-Tawaha, A. R. M. S., Pham, V. V., Nguyen, X. P. (2019). Comparative analysis on performance and emission characteristics of an in-Vietnam popular 4-stroke motorcycle engine running on biogasoline and mineral gasoline. *Renewable Energy Focus, 28,* 47–55.
14. Hoang, A. T., Nižetić, S., Ölçer, A. I. (2021). 2, 5-Dimethylfuran (DMF) as a promising biofuel for the spark ignition engine application: A comparative analysis and review. *Fuel, 285,* 119140.
15. Kalghatgi, G. T., Risberg, P., Ångström, H. E. (2006). Advantages of fuels with high resistance to auto-ignition in late-injection, low-temperature, compression ignition combustion. *SAE Technical Papers,* 2006-01-3385.
16. Kalghatgi, G. T., Risberg, P., Ångström, H. E. (2007). Partially pre-mixed auto-ignition of gasoline to attain low smoke and low NO_X at high load in a compression ignition engine and comparison with a diesel fuel. *SAE Technical Papers,* 2007-01-0006.
17. Feng, L., Sun, X., Pan, X., Yi, W., Cui, Y. et al. (2021). Gasoline spray characteristics using a high pressure common rail diesel injection system by the method of laser induced exciplex fluorescence. *Fuel, 302(3),* 121174.
18. Manente, V., Johansson, B., Cannella, W. (2011). Gasoline partially premixed combustion, the future of internal combustion engines. *International Journal of Engine Research, 12(3),* 194–208.
19. Cui, Y., Liu, H., Wen, M., Feng, L., Ming, Z. et al. (2022). Optical diagnostics of misfire in partially premixed combustion under low load conditions. *Fuel, 329(5),* 125432.
20. Sellnau, M., Sinnamon, J., Hoyer, K., Husted, H. (2011). Gasoline direct injection compression ignition (GDCI)-diesel-like efficiency with low CO_2 emissions. *SAE Technical Papers,* 2011-01-1386.
21. Cracknell, R. F., Ariztegui, J., Dubois, T., Hamje, H., Pellegrini, L. et al. (2014). Modelling a gasoline compression ignition (GCI) engine concept. *SAE Technical Papers,* 2014-01-1305.
22. Zhang, Y., Kumar, P., Pei, Y., Traver, M., Cleary, D. (2018). An experimental and computational investigation of gasoline compression ignition using conventional and higher reactivity gasolines in a multi-cylinder heavy-duty diesel engine. *SAE Technical Papers,* 2018-01-0226.
23. Sellnau, M., Foster, M., Moore, W., Sinnamon, J., Hoyer, K. et al. (2019). Pathway to 50% brake thermal efficiency using gasoline direct injection compression ignition. *SAE Technical Papers,* 2009-01-1154.
24. Weall, A., Collings, N. (2009). Gasoline fuelled partially premixed compression ignition in a light duty multi cylinder engine: A study of low load and low speed operation. *SAE Technical Papers,* 2019-01-1791.
25. Xiao, G., Zhang, Y., Lang, J., Jiang, G. (2014). Experiment of the effects of intake temperature on GCI engine combustion and emission characteristics (in China). *Transactions of CSICE, 32(2),* 125–130 (in Chinese).
26. Solaka, H., Aronsson, U., Tuner, M., Johansson, B. (2012). Investigation of partially premixed combustion characteristics in low load range with regards to fuel octane number in a light-duty diesel engine. *SAE Technical Papers,* 2012-01-0684.
27. Jiang, C., Li, Z., Liu, G., Qian, Y., Lu, X. (2019). Achieving high efficient gasoline compression ignition (GCI) combustion through the cooperative-control of fuel octane number and air intake conditions. *Fuel, 242(2),* 23–34.
28. An, Y., Tang, Q., Vallinayagam, R., Shi, H., Sim, J. et al. (2019). Combustion stability study of partially premixed combustion by high-pressure multiple injections with low-octane fuel. *Applied Energy, 248,* 626–639.

29. Goyal, H., Kook, S. (2019). Ignition process of gasoline compression ignition (GCI) combustion in a small-bore optical engine. *Fuel, 256,* 115844.
30. Liu, H., Mao, B., Liu, J., Zheng, Z., Yao, M. (2018). Pilot injection strategy management of gasoline compression ignition (GCI) combustion in a multi-cylinder diesel engine. *Fuel, 221,* 116–127.
31. Wang, H., Yao, M., Reitz, R. D. (2013). Development of a reduced primary reference fuel mechanism for internal combustion engine combustion simulations. *Energy and Fuels, 27(12),* 7843–7853.
32. Zhang, X., Wang, H., Zheng, Z., Reitz, R., Yao, M. (2016). Experimental investigations of gasoline partially premixed combustion with an exhaust rebreathing valve strategy at low loads. *Applied Thermal Engineering, 103(2014),* 832–841.
33. Zhou, L., Hua, J., Liu, F., Liu, F., Feng, D. et al. (2018). Effect of internal exhaust gas recirculation on the combustion characteristics of gasoline compression ignition engine under low to idle conditions. *Energy, 164(5),* 306–315.
34. Zhou, L., Hua, J., Wei, H., Han, Y. (2019). An experimental investigation on low load combustion stability and cold-firing capacity of a gasoline compression ignition engine. *Engineering, 5(3),* 558–567.
35. Zhu, Y., Wang, H., Zhang, X., Tong, L., Feng, H. et al. (2016). Gasoline compression ignition low-load combustion optimization based on double exhaust valve opening and injection strategy. *Transactions of CSICE, 34(5),* 415–422 (in Chinese).
36. Han, Z., Reitz, R. D. (1995). Turbulence modeling of internal combustion engines using RNG k-epsilon models. *Combustion Science and Technology, 106(4–6),* 267–295.
37. Park, S. W., Reitz, R. D. (2008). Modeling the effect of injector nozzle-hole layout on diesel engine fuel consumption and emissions. *Journal of Engineering for Gas Turbines and Power, 130(3),* 032805.
38. Amsden, A. A., O'Rourke, P. J., Butler, T. D. (1989). *KIVA-II: A computer program for chemically reactive flows with sprays*. Los Alamos: National Laboratory. LA-11560-MS.
39. Beale, J. C., Reitz, R. D. (1999). Modeling spray atomization with the Kelvin-helmholtz/Rayleigh-taylor hybrid model. *Atomization and Sprays, 9(6),* 623–650.
40. Schmidt, D. P., Rutland, C. J. (2000). A new droplet collision algorithm. *Journal of Computational Physics, 164(1),* 62–80.
41. Gonzalez, D. M., Lian, Z. W., Reitz, R. D. (1992). Modeling diesel engine spray vaporization and combustion. *SAE Technical Papers,* 920579.
42. Senecal, P. K., Pomraning, E., Richards, K. J., Briggs, T. E., Choi, C. Y. et al. (2003). Multi-dimensional modeling of direct-injection diesel spray liquid length and flame lift-off length using CFD and parallel detailed chemistry. *SAE Technical Papers,* 2003-01-1043.
43. Wang, H., Yao, M., Yue, Z., Jia, M., Reitz, R. D. (2015). A reduced toluene reference fuel chemical kinetic mechanism for combustion and polycyclic-aromatic hydrocarbon predictions. *Combustion and Flame, 162(6),* 2390–2404.
44. Sun, Y., Reitz, R. D. (2006). Modeling diesel engine NO_X and soot reduction with optimized two-stage combustion. *SAE Technical Papers,* 2006-01-0027.
45. Patterson, M. A., Kong, S. C., Hampson, G. J., Reitz, R. D. (1994). Modeling the effects of fuel injection characteristics on diesel engine soot and NO_X emissions. *SAE Technical Papers,* 940523.
46. Tang, Q., Liu, H., Li, M., Yao, M., Li, Z. (2017). Study on ignition and flame development in gasoline partially premixed combustion using multiple optical diagnostics. *Combustion and Flame, 177,* 98–108.